

Dynamic Reaction inside Co-Rotating Twin Screw Extruder. II. Waste Ground Rubber Tire Powder/Polypropylene Blends

Sung Hyo Lee, Maridass Balasubramanian, Jin Kuk Kim

Department of Polymer Science and Engineering, Division of Advanced Materials, Gyeongsang National University, 900 Jinju, Gyeongnam 660-701, Korea

Received 12 July 2006; accepted 21 December 2006

DOI 10.1002/app.26490

Published online 15 August 2007 in Wiley InterScience (www.interscience.wiley.com).

ABSTRACT: In this article, dynamic reaction of waste ground rubber tire powder/PP blends with compatibilizers is extended to commercially available waste rubber Viz. Ground rubber tire and PP for the possibility of getting recycled material with good mechanical properties. In the first part of the article it was shown that the compatibility of model material/PP blends has greatly improved. In this article, extensive studies have been carried out to study the effect of compatibilizers, *in-situ* compatibilization of immiscible waste ground rubber tire (WGRT) powder/polyolefin blends of various concentrations was investigated by means of extrusion process using a co-rotating twin screw extruder. It was observed that addition of small amounts of

compatibilizers like SEBS-*g*-MA to the blends of WGRT and PP-*g*-MA can result in better mechanical properties than the blends with isotactic PP. The blends of WGRT powder and PP-*g*-MA with compatibilizer have better adhesion than those of isotactic PP blends as revealed by the morphological studies using AFM and SEM. The betterment in properties can be attributed to the presence of functional group, maleic anhydride in PP-*g*-MA. © 2007 Wiley Periodicals, Inc. *J Appl Polym Sci* 106: 3209–3219, 2007

Key words: waste ground rubber tire; compatibilizers; twin screw extruder; functional group

INTRODUCTION

Blending recycled rubber with other polymeric materials has been an attractive alternate to disposal methods. Toughening of brittle plastics by incorporation of a small amount of WGRT (Waste Ground Rubber Tire) is a widely used commercial process.¹ The rubber forms discrete particles with diameter of about 1 μm or less. These particles act as stress concentrators initiating crazing. But its chief drawback has been the difficulties in obtaining adequate properties from the resultant blends. Efforts to develop recycled rubber/plastic blends have logically followed earlier blending research that produced both thermoplastic elastomers² and rubber-toughened plastics.³ Results of these numerous studies on virgin materials have provided criteria for a successful blend. As mentioned earlier, for efficient mixing of the constituting polymers, the two components must be thermodynamically incompatible enough to phase separate, but not so dissimilar that intimate intermixing cannot be accomplished.^{4–8}

This criterion implies that the domain size of the dispersed phase must be small so that interfacial

surface area is maximized, and the domain size leads to limits on the mismatch between the solubility parameters of the two components.^{2,4,6,8} Secondly, crosslinking of the rubber phase through processes such as “dynamic vulcanization” is required to reduce creep in TPEs and enhance the strength of toughened plastics.^{8–10} Finally, compatibilizers that act as interphase bridges between hard and soft phase are often required.¹¹ Of the various blends that have been reduced to practice, those based on the WGRT powder/PP(polypropylene) and PE(polyethylene) combination have been by far the most successful.¹²

The aim of this study is to employ the dynamic reaction process using compatibilizers to increase the miscibility behavior of incompatible WGRT/PP blends and compare it with other compatibilizers Viz. SEBS and SEBS-*g*-MA with respect to the mechanical, thermal, dynamic, rheological, and morphology properties. In is also the aim of this chapter to conclusive prove the occurrence of the dynamic reaction by stress-relaxation and contact angle studies.

EXPERIMENTAL

Materials

Ten different types of waste ground rubber tire powder/PP and five different types of waste ground

Correspondence to: J. K. Kim (rubber@gsnu.ac.kr).
Contract grant sponsor: Resource Recycling R&D Center.

TABLE I
Waste Ground Rubber Tire Powder/PP Resin Recipe

	iPP ₁	iPP ₂	iPP ₃	iPP ₄	iPP ₅	MAPP ₁	MAPP ₂	MAPP ₃	MAPP ₄	MAPP ₅
GRT	65	65	65	65	65	65	65	65	65	65
Isotactic PP	35	35	35	35	35	–	–	–	–	–
PP-g-MA	–	–	–	–	–	35	35	35	35	35
SEBS	–	5	10	–	–	–	5	10	–	–
SEBS-g-MA	–	–	–	5	10	–	–	–	5	10

rubber tire powder/PP formulations will be discussed in this study. The waste ground rubber tire powder materials used in the study and its source are as follows. The waste ground rubber tire powder was ground by wet grinding method and was supplied by Hongbok Industry, Korea. The composition of waste tire rubber are: polymer content of 48.5% with natural rubber (NR) and styrene-*co*-butadiene rubber (SBR) in 25 and 75% ratio, respectively. The other compositions of waste rubber were organic additives, carbon black and ash content 13.4%, 27.7%, and 10.4%, respectively. Other basic materials used in this study and their sources are as follows. PP-g-MA (RE 340B, SK Corporation, Korea) is PP functionalized with 0.15 wt % maleic anhydride onto the hydrocarbon chains of polypropylene main chain and isotactic PP (1088, Korea petrochemical, Korea) was purchased locally. The triblock copolymers, SEBS and SEBS-g-MA, were supplied by Shell Chemical Co. Ltd., USA. This copolymer has styrene end blocks and hydrogenated butadiene mid block reassembling an ethylene/butylene copolymer. Kraton G1652 containing about 30% wt styrene and molecular weight 79,000 g/mol was used throughout the study. SEBS-g-MA (Kraton FG1901X) is SEBS functionalized with 1.84 wt % maleic anhydride onto the hydrocarbon chains of the mid block. Its molecular weight and styrene contents are similar to those of Kraton G1652. The Table I show the formulations, which were tested with various compatibilizers.

Preparation of blends by twin screw extruder

To understand the mechanism of dynamic vulcanization process, blending of WGRT powder with polyolefins viz. isotactic PP and maleic anhydride grafted PP was studied in the presence of compatibilizers such as styrene-ethylene-butylene-styrene (SEBS) and maleic anhydride graft SEBS (SEBS-g-MA). All experiments were performed by using a modular intermeshing twin screw extruder BauTech 19 mm equipped.

Preparation of the specimens for tensile testing

The extruders were palletized and then injection molded. The test specimens pertained to ASTM

standards [dumbbell shaped samples for tensile strength and elongation at break test (ASTM D412)]. The temperature of the injection molding cylinder was kept at 235°C and the mold temperature was 30 ~ 35°C with the injection pressure at 2000 ~ 24,000 psi.

Characterizations

Stress-strain properties

Tensile testing was done on dumbbell samples using the UTM (LLOYD INSTRUMENTS, LR10K, UK) as per ASTM D412 at a crosshead speed of 50 mm/min. The test was done at room temperature. The tensile strength (MPa), elongation at break (%) and modulus at 100% were recorded automatically from the stress-strain plots. For each tensile strength reported, at least five sample measurements were averaged.

Thermal analysis

For determining the approximate composition of the TPV, thermogravimetric analysis (TGA) was carried out in a DuPont TA2100 thermo gravimetric analyzer in the temperature range of 50–700°C at a heating rate of 20°C/min. The degradation temperature as well as percent of loss of mass were calculated from the histograms.

Rheological properties

The rheological properties of the samples were studied using a capillary rheometer (model Galaxy V8052, Kayeness Inc., USA) with the length 0.591 and diameter 0.0276 in. The L/D of the capillary was 20 and measurements were carried out at 250°C. Each flow curve was generated from data collected at five different shear rates ranging from 7.5 s⁻¹ to 1500 s⁻¹.

Stress relaxation

GRT/PP blends used in stress-relaxation experiments were mechanically conditioned at 100% strain in an UTM machine. The samples were subjected to

cyclic loading and unloading until reproducible hysteresis loops were obtained. The stress in the specimen was recorded as a function of time on a moving chart paper for ~ 5 min. The stress was seen to relax at a rapid rate in the beginning and, with increasing time, the rate of stress relaxation gradually decreased. By the time the experiment was terminated, the stress had become almost constant. Ten samples of each variety were subjected to the stress-relaxation test and the average percentage stress relaxation at different times could be estimated from the curves obtained.

Contact angle

A commonly used approach to treat solid surface energies is that of expressing any surface tension as a sum of components due to dispersion forces, γ^d and polar forces, γ^p :⁸

$$\gamma = \gamma^d + \gamma^p \quad (1)$$

The interfacial tension between two phases α and β is then expressed in terms of the two component of each phase:

$$\gamma_{\alpha\beta} = \gamma_\alpha + \gamma_\beta - 2\sqrt{\gamma_\alpha^d \gamma_\beta^d} - 2\sqrt{\gamma_\alpha^p \gamma_\beta^p} \quad (2)$$

For the case of a liquid drop forming a contact angle, θ on a solid surface, the appropriate forms of eq. (2) can be combined Young's equation⁹ to give:

$$\gamma_L(\cos \theta + 1) = 2\sqrt{\gamma_S^d \gamma_L^d} + 2\sqrt{\gamma_S^p \gamma_L^p} \quad (3)$$

Since values for γ_L^d and γ_L^p are to be found in the literature for two liquids, there are two unknowns on the right of eq. (3), γ_S^d and γ_S^p , the components of the solid surface energy. The determination of these components for the solid surface therefore requires contact angle data from at least two liquids of different polarity so that simultaneous versions of eq. (3) can be solved. Polar and dispersive surface free energy can be measured from the Contact Angle Analyzer (Phoenix 300, Surface Electro Optics Co. Ltd., Korea) using software.

Morphological properties

The phase morphology of the blends was studied by a scanning electron microscopy (FE-SEM, model Philips XL 30S, Netherland) and AFM (Nanoscope IV, Veeco Instruments, Inc., USA). The prepared blend was fractured in liquid nitrogen. Because of a low contrast between the two phases, etching technique was applied in order to extract PP phase at the fracture surface. Xylene was used as the solvent for

extraction at 130 °C for 30 min and the surface was coated with gold using JFC-1100E ion sputtering device.

Recyclability and aging test for base formulation

Recyclability of these materials is one of the important characteristics for their increasingly commercial usage as they could be reprocessed several times in contrast to cured rubber. So the re-use of production waste (e.g. gate section of injection molded parts) is possible. To study the recyclability of the WGRT/PP-g-MA = 65/35 the tensile test specimens were shred and injection molded again. This procedure was repeated for 10 cycles. Thermal aging of tensile samples after each time recycle time was performed using an air oven with ventilation at 70°C. Samples were taken out after 168 h and the tensile properties were measured as described.

RESULTS AND DISCUSSION

Mechanical properties of WGRT powder/polyolefins blends

Figure 1 shows the mechanical properties of the WGRT powder with isotactic PP and maleic anhydride grafted PP blends. Tensile strength and elongation at break of the WGRT powder/PP-g-MA blends are found to be much better than those of the WGRT powder/isotactic PP blends. It can also be seen that the tensile strength of the PP-g-MA blend increases by adding SEBS and SEBS-g-MA. The increase in the tensile strength is expected as the result of PP-g-MA reacting with WGRT powder and further enhanced due to the compatibility by SEBS or SEBS-g-MA. One can also see that the tensile

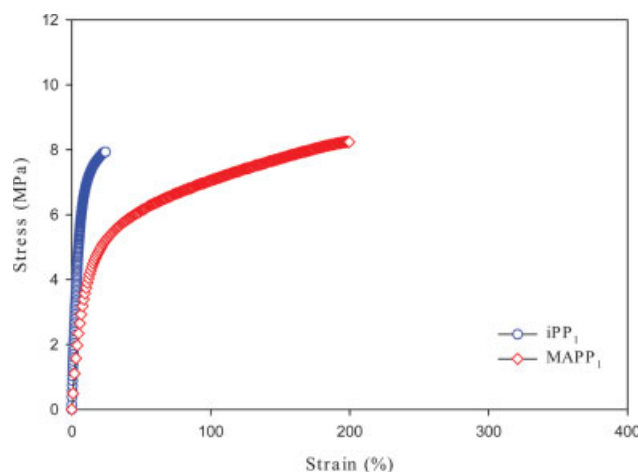


Figure 1 Mechanical properties of the WGRT powder with isotactic PP and maleic anhydride grafted PP blends. [Color figure can be viewed in the online issue, which is available at www.interscience.wiley.com.]

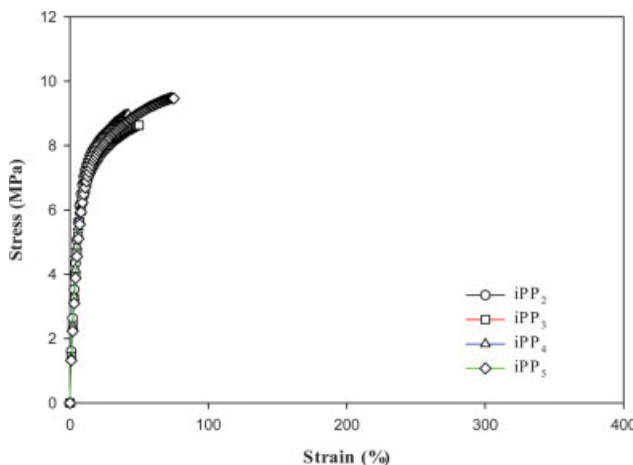


Figure 2 Mechanical properties of the WGRT powder with isotactic PP blends prepared by addition of compatibilizers. [Color figure can be viewed in the online issue, which is available at www.interscience.wiley.com.]

strengths of the WGRT/PP-*g*-MA blends are better than those of WGRT/isotactic PP blends. These WGRT powder/isotactic PP blends are simply a physical mixture of two incompatible polymers in which a continuous plastic phase is largely responsible for the mechanical properties. In this system, the large particle size and absence of adhesion is believed to be responsible for the poor properties. To get better properties, the rubber particles need to be sufficiently small and adhering to the matrix by compatibilizers and reactive functional group. Dynamic reaction of thermoplastics with the WGRT and compatibilizers increases the hardness, modulus, strength and recovery properties. As shown in Figure 2, the tensile strength of WGRT powder/isotactic

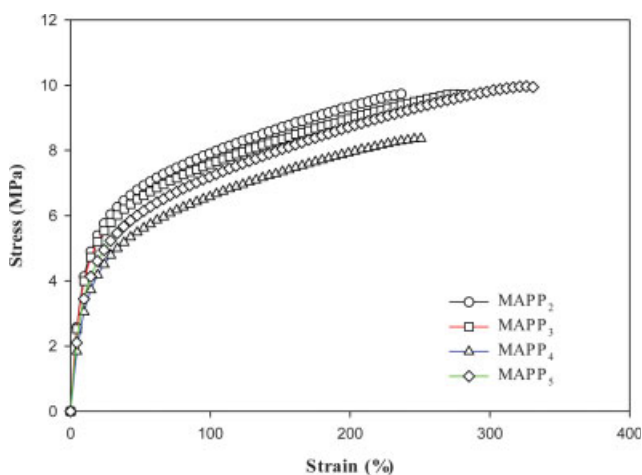


Figure 3 Mechanical properties of the WGRT powder with maleic anhydride grafted PP blends prepared by addition of compatibilizers. [Color figure can be viewed in the online issue, which is available at www.interscience.wiley.com.]

PP and PP-*g*-MA blends is improved by dynamic reaction using a kind of styrene copolymer compatibilizers. Figure 3 shows the mechanical properties of the WGRT powder with PP-*g*-MA blends prepared by addition of compatibilizers. The increases in the tensile strength is due to the enhanced compatibility by SEBS or SEBS-*g*-MA.

TGA

WGRT powder with isotactic PP and PP-*g*-MA were subjected to thermal analysis (TGA) in nitrogen (N_2). The TGA curves of the binary and ternary blends with various compositions, obtained at a heating rate of $20^\circ C/min$ are shown in Figure 4 with the corresponding parameters being given in Table II. The initial decomposition temperature and overall degradation values of all the WGRT powder based blends based on isotactic PP changed very little in comparison with PP-*g*-MA. In the WGRT powder/PP-*g*-MA blends, the 5% and 10% mass loss temperature is higher than the WGRT powder/isotactic PP blends. In this study, for the two types (PP and PP-*g*-MA) of resins two different kinds of compatibilizers (polar

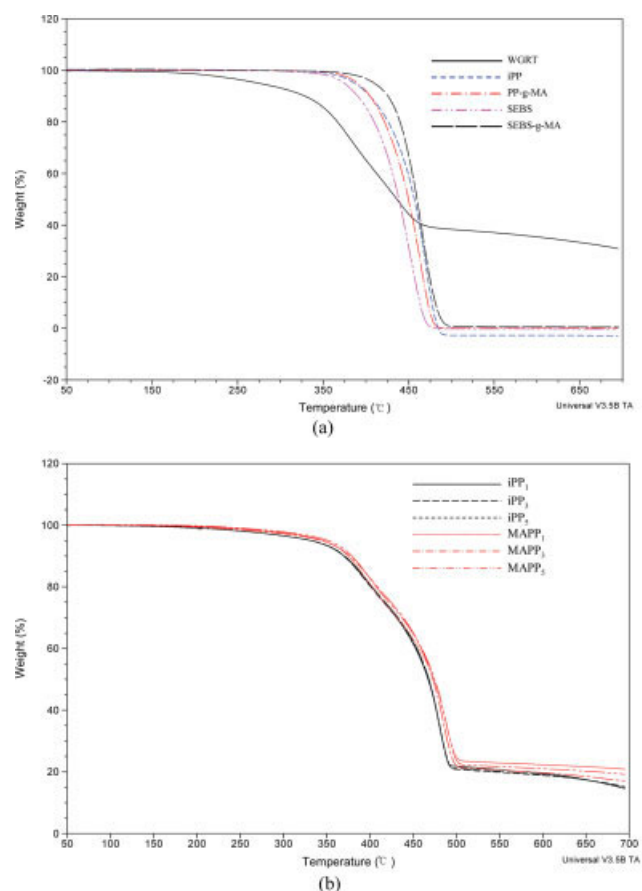


Figure 4 TGA scans of base materials and WGRT powder/PP blends. [Color figure can be viewed in the online issue, which is available at www.interscience.wiley.com.]

TABLE II
Thermogravimetric Analysis of Base Materials and
WGRT Powder/PP Blends

Sample	$T_{5\%}$ mass loss ($^{\circ}\text{C}$)	$T_{10\%}$ mass loss ($^{\circ}\text{C}$)	Temperature for maximum rate of degradation ($^{\circ}\text{C}$)
iPP	387	405	469
PP-g-MA	391	405	463
SEBS	375	390	452
SEBS-g-MA	410	426	465
WGRT	287	321	443
iPP ₁	332	370	480
iPP ₃	333	371	480
iPP ₅	333	370	480
MAPP ₁	345	375	488
MAPP ₃	344	377	484
MAPP ₅	351	380	488

and non-polar) were employed. The polar compatibilizer considered are SEBS-g-MA, while the nonpolar one is the SEBS. In the case of polar compatibilizer used for WGRT powder/PP blends, the functional polymer SEBS-g-MA gave the best thermal stability of all WGRT powder/PP blends both for isotactic PP and PP-g-MA, particularly when 10 phr of SEBS-g-MA was used. The higher thermal stability of the compound compatibilized with SEBS (MAPP₃) or SEBS-g-MA (MAPP₅) than the base compound WGRT powder/PP-g-MA (MAPP₁) can be explained by the fact that the EB midblock of the SEBS copolymer gave better compatibility with PP. It had been shown that PP has good compatibility with the EB (ethylene-*co*-butylene) block copolymer because of the repulsion effect of ethylene and butylene segments that might contribute to the improvement of the miscibility of PP with WGRT powder. All the blends based on WGRT powder started to lose mass at about 220 $^{\circ}\text{C}$.

Rheological properties

The effect of olefins on the rheological properties of the WGRT powder blends and different compatibilizers is shown in Figure 5(a,b). Figure 5(a) indicates that the shear viscosity for all the blends containing different compatibilizers has the same behavior i.e. the shear viscosity decreases as the shear rate increases. The shear viscosity of pure isotactic PP and PP-g-MA resins is shown in Figure 5(a), showing the similar behavior, although PP-g-MA is a little higher in magnitude. The shear stress as a function of shear rate is shown in Figure 5(b), exhibiting the behavior is a way that the shear stress increases as the shear rate increases for all the WGRT powder/polypropylene blends with compatibilizers. All the materials also behave in a non-newtonian manner. Therefore, it is also obvious that all the WGRT powder-based blends under study exhibited shear-thin-

ning behavior. This also attributes to the formation of chemical bond between the rubber chains and the compatibilized thermoplastics, which increases their stability toward shear breakdown during mixing, and therefore, less reduction in the shear viscosity of the blends.

Stress relaxation

Stress relaxation curves of the compositions at a strain of 100% against time is shown in Figure 6. It can be seen that the stress relaxation of WGRT powder/i-PP blend is higher when compared to the corresponding WGRT powder/PP-g-MA. With the addition of SEBS-g-MA, the same trend is seen viz. WGRT powder/i-PP/SEBS-g-MA has higher stress relaxation than the WGRT powder/PP-g-MA/SEBS-g-MA. The stress relaxation process in a polymeric material may be assumed to consist of orientation of chain units and slippage of chain segments along with dewetting of fillers from the matrix. The stress

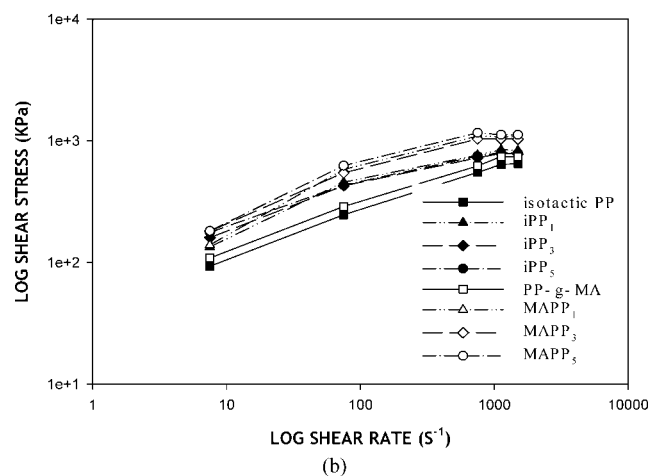
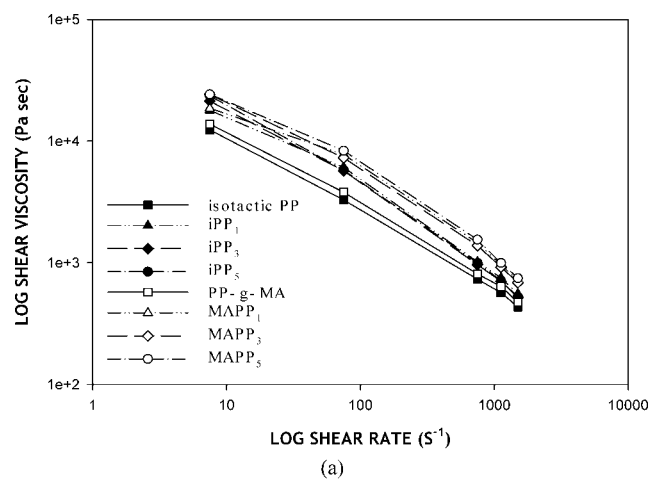


Figure 5 The effect of olefins in the WGRT powder and different compatibilizers blend on the rheological properties.

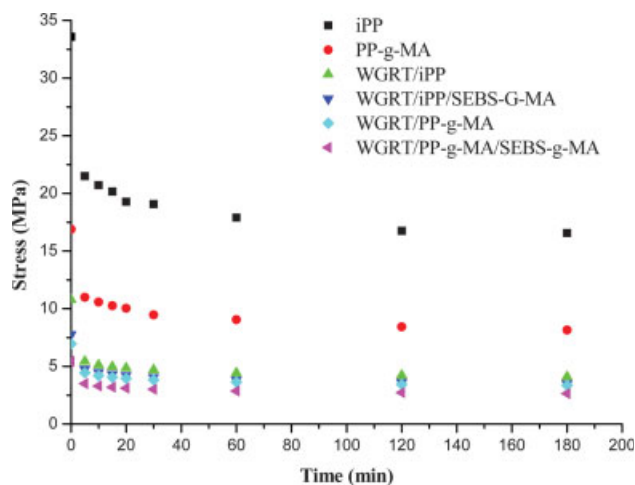


Figure 6 Stress relaxation curves of the PP and compositions at a strain of 100%. [Color figure can be viewed in the online issue, which is available at www.interscience.wiley.com.]

decay of the unfilled compound is very fast initially and very slow in the long-time region. A quantitative representation of the stress relaxation process (at room temperature, within an experimental time limit) can be made with a model consisting of two Maxwell elements and one spring, all in parallel. Then tensile modulus of the material at time t may be expressed as:¹³

$$E(t) = E_e + E_1 e^{-t/\tau_1} + E_2 e^{-t/\tau_2}$$

where E_i and τ_i represents the tensile moduli and relaxation times of the elements, respectively. The stress relaxation data have been analyzed by the curve fitting method using the commercially available software package ORIGIN 6. The moduli and relaxation times (at 100% strain) of the compositions are shown in Table III.

τ_2 for the WGRT powder/i-PP blend is very high Viz. 41 minutes as against the lower value of only 8 min for WGRT powder/PP-g-MA blends. This tremendous difference is also seen for their compatibilized counterparts.

As we can see that the SEBS-g-MA based blends have lower stress relaxation curves than when it is absent for both WGRT powder/iPP and WGRT powder/PP-g-MA blends, this gives the conclusive proof that compatibilization has occurred which is possible only by the occurrence of dynamic reaction whose mechanism has already been suggested. It also proves that the WGRT powder/PP-g-MA/SEBS-g-MA blend has more efficient dynamic reaction than the PP based counterpart due to the additional MA groups from the PP-g-MA part which takes part in the reaction.

Contact angle measurements

The occurrence of dynamic reaction will change the surface properties of the blends. Measurement of contact angle is a common method to evaluate the surface properties of polymers. This method consists of measuring the contact angle of two or more liquids on the surface of solid polymers. These liquids have known polar and dispersive components of the surface tension from specific handbooks. Then, the contact angle can be used to calculate the surface energies of the polymer. In this case, we used water and diiodomethane for the investigation and Owen-Wendt equation for analysis. The results are tabulated in Tables IV and V for the isotactic PP and PP-g-MA based blends.

From Table IV, we can see that the change in the contact angle for PP sample decreases drastically from 113° to 75° and later with the addition of SEBS and SEBS-g-MA it decreases by 2° and 3°, respectively. Also, in the case of PP-g-MA, the contact angle decreases drastically from 82° to 66° but later with the addition of SEBS it decreases by 3° similar to the PP based counterpart, but decreases very drastically by 12° on SEBS-g-MA addition. We know that the increase in the polar component in surface tension favors the enhancement of the specific interaction between the constituent polymers. Once again we see that this is the maximum in WGRT/PP-g-MA/SEBS-g-MA blend. Thus, both the results indicate conclusively the efficiency of the dynamic reaction.

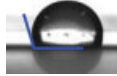





Morphological properties

The morphological changes of the WGRT powder blends with different polypropylene and their blends with different compatibilizers are shown in Figure 7(a-f). Blends with different olefins (isotactic PP & PP-g-MA) exhibited different surface morphologies, as well as those with different compatibilizers in their systems; nevertheless all exhibited two different dispersed phases due to thermodynamic incompatibility of the hard and soft segment phase. The surface morphology of the WGRT powder blends with

TABLE III
The Moduli and Relaxation Times (at 100% Strain) of the Compositions

Composition	E_1 (MPa)	τ_1 (min)	E_2 (MPa)	τ_2 (min)
Isotactic PP	7.73	8.17	7.73	0.11
PP-g-MA	3.89	9.79	3.89	0.11
WGRT/iPP	5.44	1.59	1.24	41.35
WGRT/PP-g-MA	1.65	0.05	1.65	8.41
WGRT/iPP/SEBS-g-MA	3.02	1.83	1.15	33.33
WGRT/PP-g-MA/SEBS-g-MA	0.76	0.04	2.02	2.05







TABLE IV
Results of Contact Angle Measurement for Base Materials and
WGRT Powder/iPP Based Blends

	Total surface energy (γ mJ/m ²)	Dispersive component (γ_s^d mJ/m ²)	Polar component (γ_s^p mJ/m ²)	Contact angle (θ)
Isotactic PP	37.507	36.695	0.811	113° 
SEBS	47.165	42.124	5.041	74° 
SEBS-g-MA	48.993	42.505	6.488	70° 
WGRT/iPP	50.43	43.05	7.38	75° 
WGRT/iPP/SEBS	52.56	44.38	8.18	73° 
WGRT/iPP/SEBS-g-MA	53.06	43.42	9.61	72° 

isotactic PP shows that dispersion of the rubber particles is not good [see Fig. 7(a)] as compared to PP-g-MA blend, which as expected exhibited smooth surfaces with small dispersed phases in a PP continuous matrix ([Fig. 7(d)]. With the addition of SEBS and SEBS-g-MA compatibilizers as shown in Fig. 7(e,f), the elongated dispersed phase becomes more somewhat spherical in shape in the case of both PP and PP-g-MA blends in which the dispersed particles is more visible in the continuous phase of the

matrix because of SEBS-g-MA reacting with PP and WGRT powder. The effect of SEBS-g-MA in the domain size of the WGRT dispersed phase in WGRT/PP-g-MA [Fig. 7(f)] is much smaller than that the WGRT/isotactic PP [Fig. 7(c)] blends. It is believed that the retardation of phase growth in the WGRT/PP-g-MA blend takes phase and the morphology of the WGRT/PP-g-MA blend is more stable than that of the WGRT/isotactic PP blend due to dynamic reaction during extrusion. The reaction leads to

TABLE V
Results of Contact Angle Measurement for WGRT Powder/PP-g-MA Blends

	Total surface energy (γ mJ/m ²)	Dispersive component (γ_s^d mJ/m ²)	Polar component (γ_s^p mJ/m ²)	Contact angle (θ)
PP-g-MA	41.671	38.711	2.960	82° 
SEBS	47.165	42.124	5.041	74° 
SEBS-g-MA	48.993	42.505	6.488	70° 
WGRT/PP-g-MA	52.29	41.98	10.31	66° 
WGRT/PP-g-MA/SEBS	54.04	43.53	10.51	63° 
WGRT/PP-g-MA/SEBS-g-MA	56.071	45.61	10.461	54° 

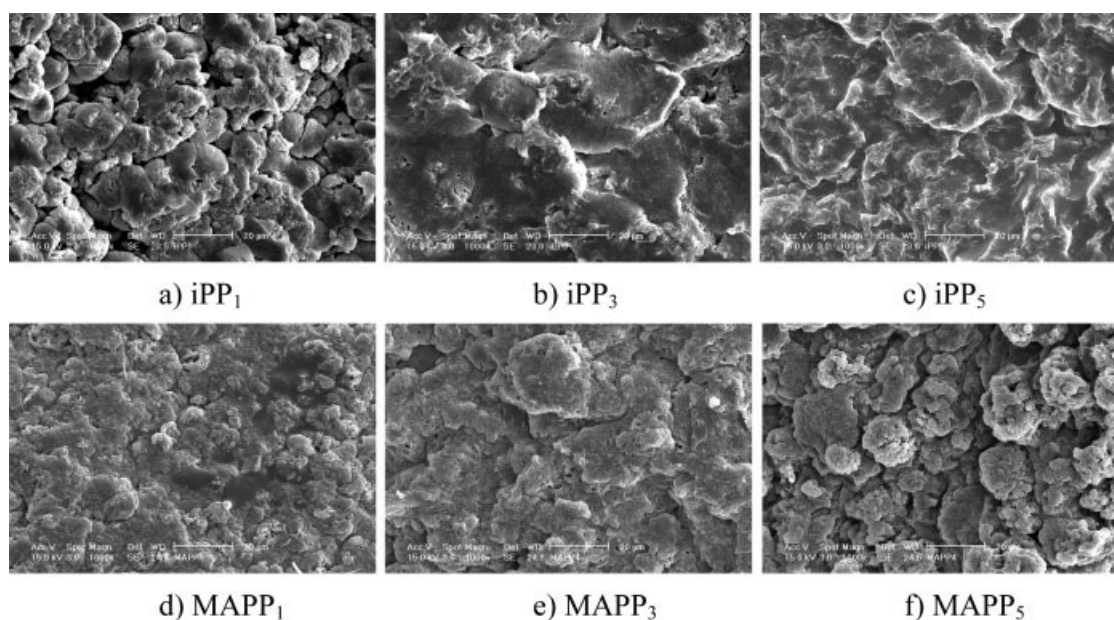


Figure 7 The morphological changes of the WGRTP powder blends with different polypropylene and different compatibilizers.

enhanced chemical interaction at the interface and improved adhesion between the two polymers. This dynamic reaction occurrence also explains the superior mechanical properties of WGRTP/PP-*g*-MA blends in comparison with the WGRTP/isotactic PP blends. The continuous hard phase and dispersed soft phase segments are clearly visible with smoother surfaces.

To investigate the morphology of all blends in more detail, the samples were etched but still not much change in the morphology was observed. Electron microscope is ambiguous to find morphological changes. Therefore, we used AFM to figure out morphological changes.

Investigation of dynamic reaction between WGRTP powder/olefins blends in the extruder

The methodology of investigation of the morphology development of WGRTP powder/PP blend along the

extruder length is similar to the one followed in previously research. A schematic description of the dynamic reaction process in the extruder is shown in Figure 8. The SEM photographs of the blends taken from the different sampling points after etching in *p*-xylene are shown in Figure 9. For the quantitative morphology analysis and in order to achieve a good contrast it was necessary to dissolve the PP matrix phase. In Figure 9, as the distance from the hopper to die increase, the initial rubber matrix/PP domain is changed into PP matrix/rubber domain along the screw position¹⁴ and confirms that significant changes in morphology occur during the melting process.

We believe AFM is able to figure out dynamic reaction between the two polymers. In Figure 10 (scale 4), AFM phase image of 65/35 WGRTP powder/PP blends image is shown. The dispersed WGRTP powder is the bright phase while dispersed compatibilizer is dark-bright phase dispersed in the

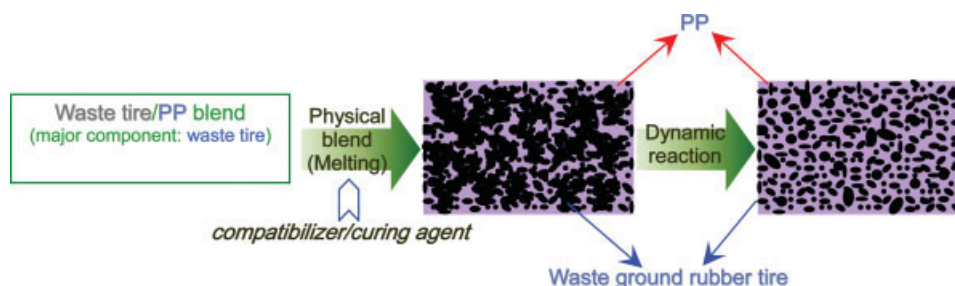


Figure 8 A schematic description of dynamic reaction process. [Color figure can be viewed in the online issue, which is available at www.interscience.wiley.com.]

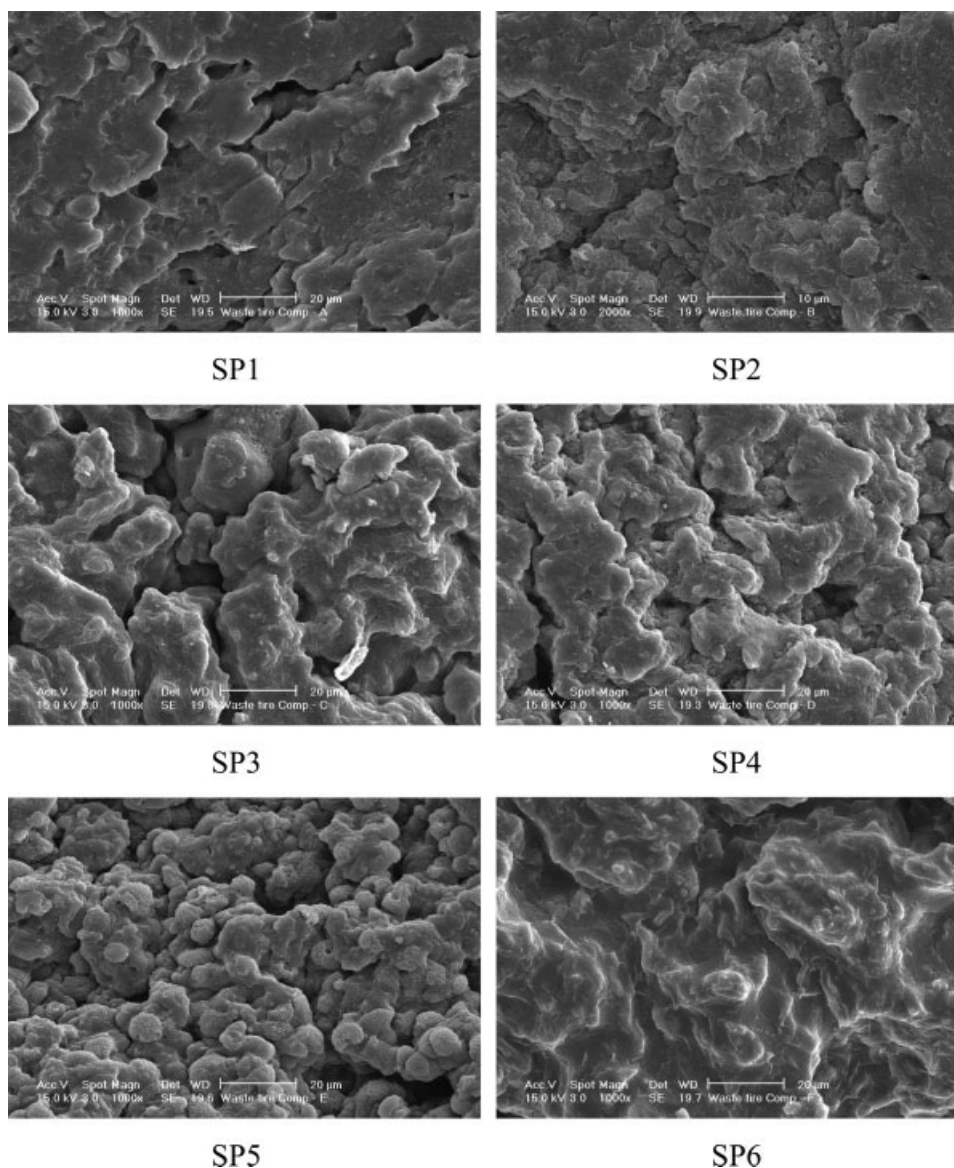


Figure 9 SEM photographs a rubber phase are changed to rubber domain at rubber matrix along the screw position.

dark phase PP matrix.¹⁵ In case of iPP_3 and iPP_5 blends shown in Figure 10, dark-bright phase (compatibilizers) forms a larger distribution compared to $MAPP_3$ and $MAPP_5$ blends. It also means that the compatibilizers are thermodynamically not very much compatible with isotactic PP. On the contrary, the dark-bright phase in $MAPP_3$ and $MAPP_5$ suggests the domain size is very fine and hence good compatibility of the constituent polymers. From this microscope graphs, we can draw the schematic drawing which is shown Figure 11.

Recyclability and thermal aging test of $MAPP_1$

As shown in Figure 12, surprisingly the reprocessing had little effect on the tensile properties of the

WGRT powder/PP-g-MA blends. In the case of $MAPP_1$, the elongation at break showed a decrease of 10% and an increase of 0.5 MPa in tensile strength after ten cycles. All specimens are hardened after thermal aging due to migration of low molecular weight such as process oil. Therefore, all of the formulation based on WGRT powder/PP-g-MA such as $MAPP_1$ to $MAPP_5$ retain their properties well and can be recycled at least 10 times.

In Figure 12 the tensile properties after thermal aging at 70°C are shown. The values of elongation at break changed marginally. The tensile strength showed a slight increase for all cycle times after 168 h of aging. In general all the formulations investigated were found to be remarkably stable against thermal aging.

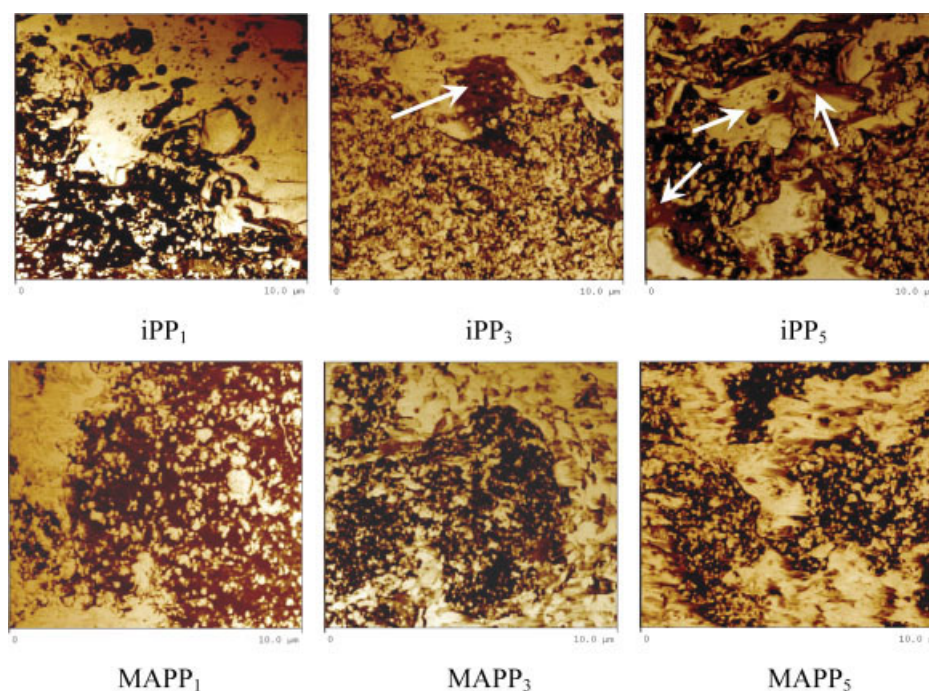


Figure 10 The effect of compatibilizer on the interface morphology in the AFM (scale 10 μm). [Color figure can be viewed in the online issue, which is available at www.interscience.wiley.com.]

CONCLUSIONS

This article demonstrated the dynamic reaction process in WGRT powder with different types of olefins in the presence of different compatibilizers occurring inside a twin screw extruder. The blends of WGRT and PP-g-MA with the addition of SEBS-g-MA gave better mechanical properties than the blends with isotactic PP. A similar phenomena but to a lesser extent was observed for model material/PP-g-MA blends in the presence of SEBS-g-MA compatibilizer as discussed in previous paper. The mechanical properties of WGRT with different olefins (isotactic polypropylene and maleic anhydride grafted polypropylene) are lower than those with addition of compatibilizers such as SEBS and SEBS-g-MA. The

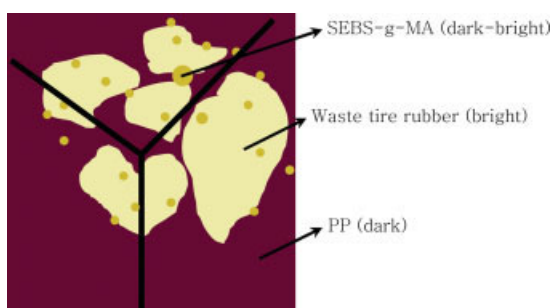


Figure 11 Schematic separation phases in the WGRT/PP/compatibilizers blend. [Color figure can be viewed in the online issue, which is available at www.interscience.wiley.com.]

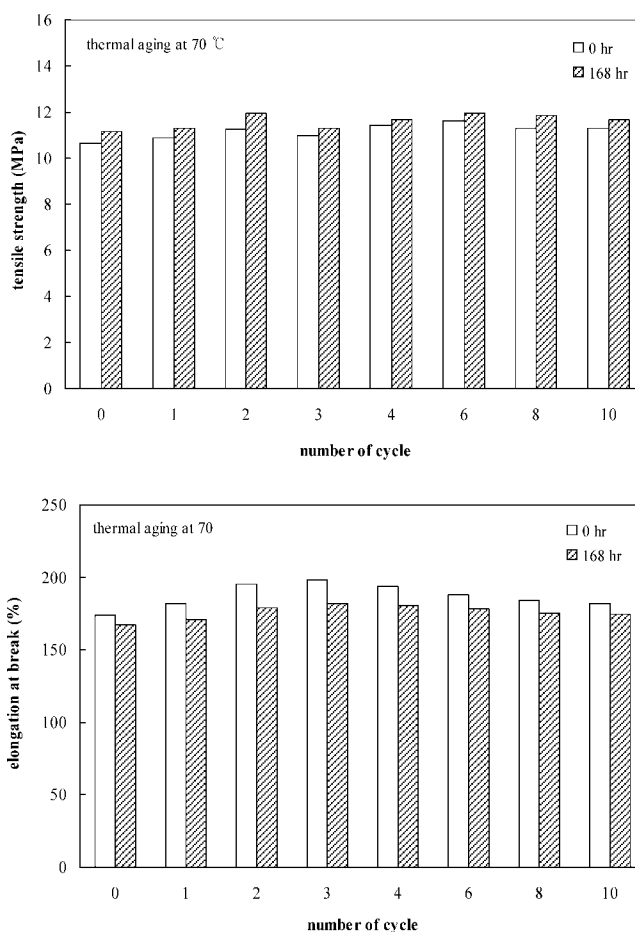


Figure 12 Influence of recycling and thermal aging on tensile properties of WGRT/PP-g-MA (MAPP₁).

blends of WGRT powder and different olefins are simply a physical mixture of two incompatible polymers in which a continuous plastic phase is largely responsible for the mechanical properties. The large particle size of WGRT and the poor adhesion are believed to be liable for the poor properties. However, with the addition of SEBS-*g*-MA in the blends, there is a drastic improvement in the mechanical properties, which is due to the presence of reactive functional group of maleic anhydride of SEBS undergoing dynamic reaction with PP during melt processing. There is no significant change in the rheological properties for all the blends. It showed that thermoplastic elastomer exhibited shear thinning behavior, which follows the power law model over the entire range of the shear rates. The surface morphology of WGRT/isotactic PP blends shows elongated dispersed phase of rubber particles while those blends with PP-*g*-MA exhibits a smooth surface with relatively small dispersed phases in a continuous matrix. However, with the addition of SEBS-*g*-MA compatibilizer, the elongated phase of WGRT/isotactic PP blends becomes spherical in shape and those with PP-*g*-MA the surface becomes smoother and the dispersed particles are more clearly visible.

The blends of WGRT powder and PP-*g*-MA with compatibilizer have better adhesion than those of isotactic PP blends as revealed by the AFM results due to the presence of functional group, maleic an-

hydride in PP-*g*-MA. Recyclability studies revealed that the tensile properties were retained even after 10 cycles.

References

1. Bucknall, C. B. Appl Sci Publishers London, 1977.
2. Coran, A. Y. In Handbook of Elastomer-New Development and Technology; Bhowmick, A. K.; Stephens, H. L., Eds.; Dekker: New York, 1987.
3. Newman, S. In Polymer Blends; Paul, D. R.; Newman, S., Eds.; Academic Press: New York, 1978.
4. Stehling, F. C.; Huff, T.; Speed, C. S.; Wissler, G. J Appl Polym Sci 1981, 26, 2693.
5. Jang, B. Z.; Uhlmann, D. R.; Vander Sande, J. B. J Appl Polym Sci 1985, 30, 2485.
6. Jordhamo, G. M.; Manson, J. A.; Sperling, L. H. Polym Eng Sci 1986, 26, 517.
7. Ho, R. M.; Wu, C. H.; Su, A. C. Polym Eng Sci 1990, 30, 511.
8. Lohse, D. J.; Garner, R. T.; Graessley, W. M.; Krishnamoorti, R. Rubber Chem Technol 1999, 72, 569.
9. Kunz-Douglass, Beaumont, P. W. R.; Ashby, M. F. J Mater Sci 1980, 15, 1109.
10. Coran, A. Y.; Patel, R. P. In Thermoplastic Elastomers; Holden, G.; Legge, N. R.; Quirk, R. P.; Schroeder, H. E., Eds.; Hanser/Gardner: Cincinnati, 1996.
11. Phan, T. T. M.; DeNicola, A. J.; Schadler, L. S. J Appl Polym Sci 1998, 68, 1451.
12. Coran, A. Y.; Patel, R. P. Rubber Chem Technol 1980, 53, 141.
13. Sabia, R.; Eirich, F. R. J Polym Sci Part A 1963, 1, 2497.
14. Fukumori, K.; Sato, N. IRC 2005 Yokohama, Japan, Oct. 24–27, 2005.
15. Radovanovic, E.; Carone, E., Jr.; Goncalves, M. C. Polym Test 2004, 23, 231.